

Correlated charge polarization in a chain of coupled quantum dots

R. Kotlyar

Department of Physics, University of Maryland, College Park, Maryland 20742-4111

C. A. Stafford

Fakultät für Physik, Albert-Ludwigs-Universität, D-79104 Freiburg, Germany

S. Das Sarma

Department of Physics, University of Maryland, College Park, Maryland 20742-4111

(Received 22 May 1998)

Coherent charge transfer in a linear array of tunnel-coupled quantum dots, electrostatically coupled to external gates, is investigated using the Bethe ansatz for a symmetrically biased Hubbard chain. Charge polarization in this correlated system is shown to proceed via two distinct processes: formation of bound states in the metallic phase, and charge-transfer processes corresponding to a superposition of antibound states at opposite ends of the chain in the Mott-insulating phase. The polarizability in the insulating phase of the chain exhibits a universal scaling behavior, while the polarization charge in the metallic phase of the model is shown to be quantized in units of $e/2$. [S0163-1829(98)52228-X]

Tunneling of a single electron from one region to another in a mesoscopic system leads to a modification of the dielectric response of the system¹ that can be detected via single-electron capacitance spectroscopy.² Capacitance measurements allow one to study charge transfer *in equilibrium*, and thus provide an important alternative to transport measurements³⁻⁶ in probing the effects of coherent tunneling. In this paper, we investigate the charge polarization of a linear array of tunnel-coupled quantum dots embedded between the plates of a capacitor (Fig. 1). The quantum corrections to the classical two-terminal capacitance of the system are shown to exhibit sharp resonances whose structure reveals directly the spatial correlations of the interacting many-body ground state of the system. We find that the localized character of the many-body states in the Mott-insulating phase of the model leads to extremely sharp capacitance resonances, which obey a universal scaling form analogous to the conductivity of the system.⁷ On the other hand, the extended quantum states in the metallic phase of the model are shown to lead to fractional charge transfer in some regimes of electron density, in contrast to the integer charge transfer predicted in Ref. 1.

The integrability of one-dimensional (1D) quantum many-body systems with open boundary conditions was first established⁸ for the one-dimensional Hubbard model. The Bethe ansatz solution was recently extended to include boundary potentials,⁹ and the spectrum of bound states for a single attractive boundary potential has very recently been investigated.¹⁰ Here, we investigate a Hubbard chain with equal and opposite boundary potentials at each end, which serves as a model of a capacitively biased 1D array of quantum dots. In addition to the bound states found for the case of a single boundary potential,¹⁰ we find charge-transfer states, which are quantum-mechanical superpositions of antibound states at opposite ends of the chain. These charge-transfer states are shown to dominate the polarizability in the Mott-insulating phase of the model.

We consider a closed linear system of quantum dots coupled electrostatically to bias gates and a backgate (Fig. 1). The backgate allows the system to be charged with N excess electrons, this excess charge being shared among the dots in the chain by quantum-mechanical tunneling. We describe this coupled quantum dot chain by the Hubbard model¹¹ in the experimentally accessible limit when the interdot capacitances are negligible compared to the capacitances C_g to the external gates. The Hamiltonian of the system, including the work done by the external voltage sources, is

$$H = -t \sum_{\sigma} \sum_{i=1}^{L-1} (c_{i+1\sigma}^{\dagger} c_{i\sigma} + \text{H.c.}) + \frac{U}{2} \sum_{i=1}^L \rho_i^2 - C_0 V^2 / 2 + \frac{eV}{2} (\rho_L - \rho_1), \quad (1)$$

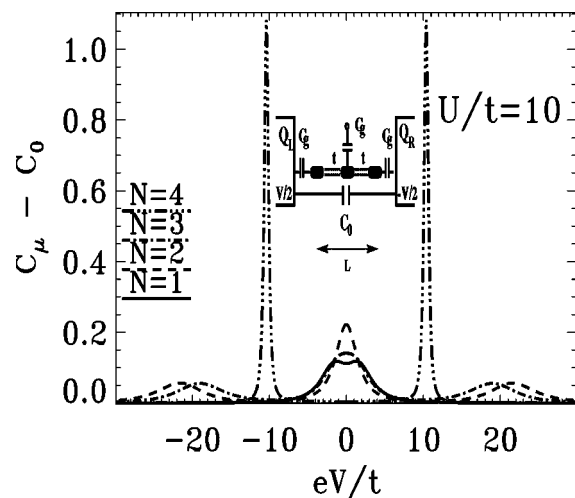


FIG. 1. The quantum corrections to the capacitance plotted in units of e^2/t of a chain of four quantum dots as a function of the bias voltage V . The number of excess electrons in the chain and the interaction strength are as indicated in a legend. Inset: The equivalent circuit of the quantum dot array under study.

TABLE I. Complex roots of Eqs. (4) and (5) (with exponential accuracy as $L \rightarrow \infty$) corresponding to the bound and antibound states present in the ground state of Eq. (1), as a function of the bias V . Here $eV_1 = U/2 + [(U/2)^2 + 4t^2]^{1/2}$ and $eV_2 = U + [U^2 + 4t^2]^{1/2}$. In the insulating phase of the model ($N=L$), polarization of the system proceeds via transfer of the antibound state k_{L-1} from one end of the array to the other at the boundary of regions I and II. In the metallic phase, polarization of the system proceeds via the successive trapping of electrons on the boundary dot with attractive potential at the onset of regions I and III.

	I	II	III
	$2t/e < V < V_1$	$V_1 < V < V_2$	$V > V_2$
	$k_L = i \ln(eV/2t)$	$k_L = i \ln(eV/2t)$	$k_L = i \ln(eV/2t)$
$N=L$	$k_{L-1} = \pi - i \ln(eV/2t)$	$k_{L-1} = \pi + i \sinh^{-1}(i \sin k_L + U/2t)$	$k_{L-1} = -i \sinh^{-1}(i \sin k_L + U/2t)$
		$\lambda_M = \sin k_L - iU/4t$	$\lambda_M = \sin k_L - iU/4t$
	$k_N = i \ln(eV/2t)$	$k_N = i \ln(eV/2t)$	$k_N = i \ln(eV/2t)$
$N < L$		$\lambda_M = \sin k_N - iU/4t$	$k_{N-1} = -i \sinh^{-1}(i \sin k_N + U/2t)$
			$\lambda_M = \sin k_N - iU/4t$

where $c_{i\sigma}^\dagger$ creates an electron of spin σ on dot i , $\rho_i = \sum_{\sigma} c_{i\sigma}^\dagger c_{i\sigma}$, $U = e^2/C_g$ is the charging energy of a quantum dot, and C_0 is the classical geometrical capacitance between the left and right gates. Equation (1) can be considered as a phenomenological Hamiltonian to describe, e.g., collective effects in a linear array of L coherently coupled quantum dots, which are electrostatically defined in a two-dimensional electron gas by means of metallic gates on top of a GaAs/Al_xGa_{1-x}As heterostructure.¹¹ Here we consider only the single electronic orbital in each quantum dot that lies nearest the Fermi energy. This approximation should be adequate¹¹ to describe collective charging effects in the regime where the interdot conductance $G < e^2/h$. Equation (1) is the prototypical minimal model of correlated fermions on a lattice, and describes, e.g., the correlation-induced metal-insulator transition.⁷ The new feature investigated here is the nonperturbative effect of the external bias (V) described by the last term in Eq. (1), which polarizes the system. Unlike previous investigations of the charge response of the system,⁷ we do not treat the bias V as a weak perturbation, but consider arbitrarily large values of V , leading to a finite transfer of charge across the chain. The polarization charge Q induced on the external capacitor plates characterizes the measurable dielectric response of the system. At zero tem-

perature, the expectation value of the polarization charge is given by

$$\langle Q \rangle = \langle Q_L - Q_R \rangle / 2 = -\partial E_0 / \partial V, \quad (2)$$

where Q_L (Q_R) is the polarization charge on the left (right) capacitor plate and E_0 is the minimum eigenvalue of Eq. (1). The two-terminal capacitance of the device is defined as $C_\mu = -\partial^2 E_0 / \partial V^2$. These quantities can be exactly obtained for the quantum dot chain using the Bethe ansatz technique, as described below.¹²

The eigenvalues of Eq. (1) may be expressed as

$$E = -2t \sum_{j=1}^N \cos k_j - C_0 V^2 / 2, \quad (3)$$

where the pseudomomenta k_j are a set of N distinct numbers that satisfy the coupled equations

$$S_V(k_j) e^{i2k_j(L+1)} = \prod_{\beta=1}^M \frac{\sin k_j - \lambda_\beta + iU/4t}{\sin k_j - \lambda_\beta - iU/4t} \frac{\sin k_j + \lambda_\beta + iU/4t}{\sin k_j + \lambda_\beta - iU/4t}, \quad (4)$$

$$\prod_{j=1}^N \frac{\lambda_\alpha - \sin k_j + iU/4t}{\lambda_\alpha - \sin k_j - iU/4t} \frac{\lambda_\alpha + \sin k_j + iU/4t}{\lambda_\alpha + \sin k_j - iU/4t} = \prod_{\beta(\neq\alpha)=1}^M \frac{\lambda_\alpha - \lambda_\beta + iU/2t}{\lambda_\alpha - \lambda_\beta - iU/2t} \frac{\lambda_\alpha + \lambda_\beta + iU/2t}{\lambda_\alpha + \lambda_\beta - iU/2t}, \quad (5)$$

where λ_α , $\alpha = 1, \dots, M$ are a set of distinct numbers referred to as spin rapidities, and

$$S_V(k_j) = \frac{1 - (eV/2t)^2 e^{-2ik_j}}{1 - (eV/2t)^2 e^{2ik_j}} \quad (6)$$

is the single-electron scattering matrix associated with the boundary potentials.

The capacitive response of a chain of four quantum dots, calculated from Eqs. (2)–(6), is shown in Fig. 1 for several

values of N . The polarization induced by the external bias V leads to a transfer of charge across the system, which is reflected in the appearance of complex roots of the Bethe ansatz equations, corresponding to bound and antibound states on the boundary dots (see Table I). Let us first consider the Mott-insulating phase of the system, which occurs^{7,11} for commensurate electron density $N=L$. For low bias $eV < 2t$, the Bethe ansatz ground state contains only real pseudomomenta, and the charge distribution remains essentially symmetric. For $2t < eV \leq U$, a bound state forms on

the leftmost dot, characterized by the complex pseudomomentum k_L . However, due to the incompressibility of the Mott insulator, an antibound state on the rightmost dot is also filled (k_{L-1}), and there is thus no net transfer of charge. The Mott-Hubbard gap is reflected in the suppression of the low-bias capacitance (the dash-triple-dotted curve in Fig. 1). For a bias larger than the Mott-Hubbard gap, however, it becomes energetically favorable to depopulate the antibound state on the rightmost dot and populate an antibound state in the upper Hubbard band on the leftmost dot (region II in Table I). The pseudomomentum of this antibound state contributes $-2t \cos k_{L-1} = [(U - eV/2)^2 + 4t^2]^{1/2} \approx U - eV/2$ to the ground-state energy in Eq. (3) (plus small backflow terms), indicating the presence of a second electron on the leftmost dot. The resulting transfer of an electron across the array leads to a sharp capacitance resonance at $eV = eV_1 \approx U$ in Fig. 1. Finally, for $eV > eV_2 \approx 2U$, this antibound state becomes a bound state.

In order to elucidate the nature of the charge-transfer resonance in the Mott insulator, let us first consider the simplest case $L=2$, for which Eq. (1) reduces to a simple 4×4 matrix. The polarization charge and capacitance may then be obtained directly [neglecting terms of order $(t/U)^2$],

$$\frac{Q - C_0 V}{e} = \frac{1}{2} + \frac{1}{2} \frac{eV - U}{\sqrt{8t^2 + (U - eV)^2}}, \quad (7)$$

$$C_\mu - C_0 = \frac{4e^2 t^2}{[8t^2 + (U - eV)^2]^{3/2}}. \quad (8)$$

Equations (7) and (8) predict a charge transfer of e across the chain and a capacitance peak at $eV = U$. Equation (8) was obtained previously in Ref. 1, where it was shown to describe charge transfer between two arbitrary mesoscopic systems coupled weakly by tunneling. Following the above argument on the nature of charge transfer in the Mott insulator, one may expect a result analogous to Eq. (8) to hold for larger chains as well, since the effective coupling of the boundary dots via the intervening Mott insulator should decrease exponentially with system size. Indeed, the capacitance peaks at $eV \approx U$ are found to become increasingly high and narrow (the area, which corresponds to the total charge transferred, is conserved) as L increases, but their shape is found to be described very well by Eq. (8), with t replaced by an effective charge-transfer matrix element t_{eff} , as shown in Fig. 2(a). Fitting the calculated capacitance to Eq. (8), the effective charge-transfer matrix element is found to have the form

$$t_{\text{eff}} \approx t e^{-(L-2)/\xi(U/t)} \quad (9)$$

as shown in Fig. 2(b), where the correlation length ξ in the Mott-insulating phase of the 1D Hubbard model is given by⁷

$$1/\xi(U/t) = \frac{4t}{U} \int_1^\infty dy \frac{\ln(y + \sqrt{y^2 - 1})}{\cosh(2\pi t y/U)}. \quad (10)$$

Equation (9) indicates that the effective charge-transfer matrix element, which characterizes the resonant polarizability of the Mott insulator, exhibits a finite-size scaling analogous to the conductivity of the system, which also decreases exponentially with system size in the Mott insulator.⁷ t_{eff} is in

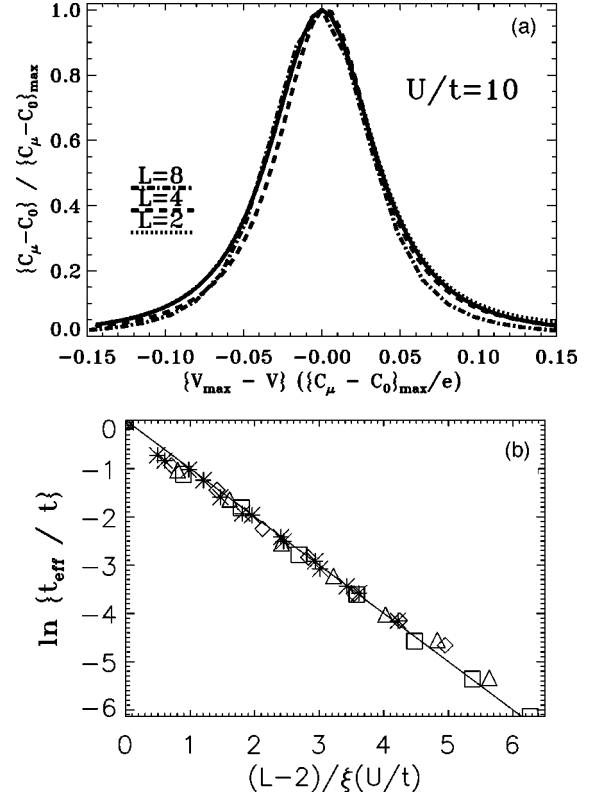


FIG. 2. (a) The charge transfer-induced resonant capacitance peaks for Mott-insulating chains of two, four, and eight dots (plotted as indicated in a legend), varying by several orders of magnitude in height and width, are shown to collapse on the rescaled capacitance peak given by Eq. (8) (solid line). (b) The effective coupling t_{eff} between the boundary dots of the Mott-insulating L -dot chains is plotted for $U/t=6, 7, 8, 9$, and 10 . The solid line with slope minus unity is shown to emphasize the scaling of the data given by Eq. (9).

fact related to the equal-time Green's function $t_{\text{eff}} = tG(1, L) = t \sum_{\sigma} \langle 0 | c_{1\sigma}^\dagger c_{L\sigma} | 0 \rangle$, and it has already been argued⁷ that G has the same scaling form as the conductivity for another choice of boundary conditions. Dielectric measurements thus present the intriguing possibility to study experimentally the correlation length of a Mott insulator formed in a coherent system of quantum dots.

While the charge-transfer resonances in the Mott-insulating phase of the model can be described by the theory of Ref. 1, it is evident from Fig. 1 that the capacitance in the metallic phase of the model, which may exhibit a low-bias double peak structure, cannot in general be described by an equation of the form of Eq. (8). As shown in Fig. 3, this double peak structure in the dilute metallic phase of the system is accentuated with increasing system size, and corresponds to a polarization charge with well-defined plateaus quantized in units of $e/2$, unlike the integer charge transfer described by Eq. (7). From Table I, we see that the polarization of the system in the metallic phase proceeds via the successive capture by the boundary dot of electrons from the Luttinger liquid states delocalized along the chain (since the antibound states are empty for $N < L$), the first at $eV = 2t$ and the second at $eV = eV_2 \approx 2U$. The breakdown of Eqs. (7) and (8) is due to the fact that the system can no longer be

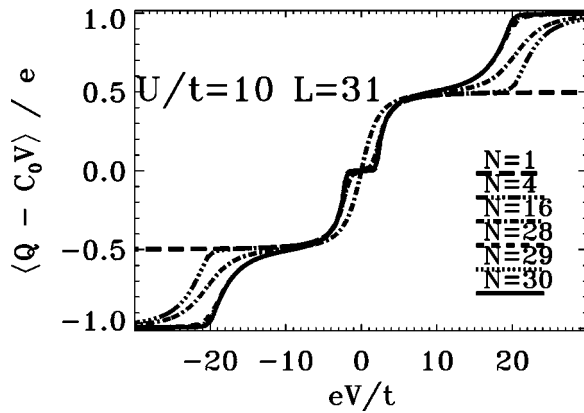


FIG. 3. Quantum correction to the polarization charge induced on the external capacitor plates versus bias voltage for a Hubbard chain of quantum dots in the metallic phase ($N < L$). Note that Q is quantized in units of $e/2$ ($N \ll L$ or $N \approx L$) reflecting a fractional ($e/2$) charge transfer within the chain.

divided into just two weakly coupled subsystems, as was assumed in Ref. 1, but instead becomes one coherent whole in the metallic phase.

The fractional increments of polarization charge shown in Fig. 3 arise because the trapping of an electron from the gapless quantum states in the central part of the array leads to an effective charge transfer over only half the system. Due to the breaking of particle-hole symmetry in the metallic phase of the model, the formation of a bound state at one end of the array need not occur at the same bias voltage as the formation of an antibound state at the other end of the array; the polarization charges on the first and L th dots are therefore no longer equal and opposite in the metallic phase, as was the case in the Mott-insulating phase. As seen in Fig. 3, the charge fractionalization near zero bias occurs for low electron densities ($N/L \ll 1$) or for a small density of holes in the Mott insulator ($1 - N/L \ll 1$). For intermediate densities, the plateau at zero bias is suppressed (see curve for $N = 16$ in Fig. 3). For $N = 1$, the physics is simple: From Table I, we see that the electron becomes bound at opposite ends of the array for $eV = \pm 2t$; for $eV \ll 2t$, the polarization of the system is negligible, leading to a plateau in the polarization charge $\langle Q \rangle$. For a dilute system with $N \ll L$, this qualitative picture remains true (see curve for $N = 4$ in Fig. 3), but for intermediate densities (see curve for $N = 16$ in Fig. 3) this single-particle picture breaks down and the charge plateau

near zero bias is suppressed. On the other hand, for $1 - N/L \ll 1$, the system behaves like a dilute gas of *holons*,⁷ the charge excitations of the strongly correlated Mott insulator, and the reappearance of the charge plateau near zero bias can be understood in terms of the trapping of holons by the boundary potentials.

Let us comment on some of the idealizations employed in the above calculation. The introduction of an interdot capacitance, neglected in Eq. (1), leads to longer ranged site-off-diagonal interactions in the array, and a smoother distribution of the externally applied voltage drop. Such an extended Hubbard model is no longer integrable via the Bethe ansatz technique, but Lanczos direct diagonalization investigations¹² indicate that the physics is qualitatively similar to that described here. Disorder, neglected in the present treatment, is not found to modify our main conclusions, as confirmed by our Lanczos investigations.¹² The scaling form of the capacitance [Eqs. (8) and (9)] in the Mott insulating phase of the system is preserved provided the disorder is not sufficiently strong to lead to a compressible state, although the correlation length ξ is found to depend on disorder. Similarly, the fractional polarization charge plateaus shown in Fig. 3 are robust with respect to disorder, though the voltage bias of the steps may be shifted. We also remark that for temperatures $k_B T$ much larger than the effective charge-transfer matrix element, the form of the capacitance peaks given in Eq. (8) and Fig. 3 will be replaced by a simple derivative of the Fermi function, of width $k_B T$; however, the peak positions can still be used to distinguish between metallic and Mott-insulating behavior.

In conclusion, we have investigated coherent charge transfer in a strongly correlated artificial linear molecule of tunnel-coupled quantum dots. The polarizability in the Mott-insulating phase of the system was found to exhibit a universal scaling form analogous to the conductivity of the system, while the polarization charge in the dilute metallic phase of the system was found to be quantized in units of $e/2$. Equilibrium charge-transfer measurements present an intriguing alternative to transport measurements to characterize the electronic states of ultrasmall structures. We believe that capacitance measurements carried out in carefully fabricated quantum dot chains should be able to observe the charge-transfer resonances and the universal scaling behavior as well as the metallic charge fractionalization phenomenon predicted here.

This work was supported by the US-ONR.

¹M. Büttiker and C. A. Stafford, Phys. Rev. Lett. **76**, 495 (1996).

²R. C. Ashoori *et al.*, Phys. Rev. Lett. **68**, 3088 (1992); **71**, 613 (1993).

³L. P. Kouwenhoven *et al.*, Phys. Rev. Lett. **65**, 361 (1990); D. Dixon *et al.*, Phys. Rev. B **53**, 12 625 (1996); R. H. Blick *et al.*, *ibid.* **53**, 7899 (1996).

⁴F. R. Waugh *et al.*, Phys. Rev. Lett. **75**, 705 (1995).

⁵N. C. van der Vaart *et al.*, Phys. Rev. Lett. **74**, 4702 (1995); F. Hofmann *et al.*, Phys. Rev. B **51**, 13 872 (1995).

⁶A. Yacoby, M. Heiblum, D. Mahalu, and H. Shtrikman, Phys. Rev. Lett. **74**, 4047 (1995).

⁷C. A. Stafford and A. J. Millis, Phys. Rev. B **48**, 1409 (1993).

⁸H. J. Schulz, J. Phys. C **18**, 581 (1985).

⁹H. Asakawa and M. Suzuki, J. Phys. A **29**, 225 (1996).

¹⁰G. Bedürftig and H. Frahm, J. Phys. A **30**, 4139 (1997).

¹¹C. A. Stafford and S. Das Sarma, Phys. Rev. Lett. **72**, 3590 (1994); R. Kotlyar and S. Das Sarma, Phys. Rev. B **55**, 10 205 (1997); C. A. Stafford and S. Das Sarma, Phys. Lett. A **230**, 73 (1997).

¹²R. Kotlyar, C. A. Stafford, and S. Das Sarma (unpublished); R. Kotlyar, Ph.D. thesis, University of Maryland, 1998.